Chinese Journal of Aeronautics, (2016), 29(3): 754–762

Chinese Society of Aeronautics and Astronautics
& Beihang University

Chinese Journal of Aeronautics

cja@buaa.edu.cn
www.sciencedirect.com

Hierarchical space–time block codes signals classification using higher order cumulants

Ling Qing [a], Zhang Limin [a,*], Yan Wenjun [a], Kong Dongming [b]

[a] Institute of Information Fusion, Naval Aeronautical and Astronautical University, Yantai 264001, China
[b] Equipment of Navy, Taiyuan 030027, China

Received 31 August 2015; revised 18 December 2015; accepted 24 January 2016
Available online 7 May 2016

KEYWORDS

Blind classification;
Fourth-order cumulants;
Multiple input single output;
Non-cooperative context;
STBCs

Abstract An efficient method for blind classification of space–time block codes (STBCs) based on fourth-order cumulants is proposed for a single receiver antenna. This paper presents a model of received STBCs signals in multiple input single output (MISO) communication systems and applies the characteristics of coding matrices to derive analytical expressions for the fourth-order cumulants to be used as the basis of an algorithm. The fourth-order cumulants at various delay vectors present non-null values that depend on the transmitted STBCs. Tests of nullity are accomplished by hypothesis testing. The proposed algorithm avoids the need for a priori information of modulation scheme, channel coefficients, and noise power. Consequently, it is well suited for non-cooperative scenarios. Simulations show that this method performs well even at low signal-to-noise ratios (SNRs).

1. Introduction

Obtaining signal parameters of the intercepted signals is a key step between signal detection and signal decoding in non-cooperative scenarios. Signal parameters include modulation scheme, channel coding information and code parameters. In recent years, the traditional blind classification of signal parameters, including interference identification, signal confirmation, radio surveillance and spectrum monitoring, has been extended to both military and commercial applications. Array signals can be employed to estimate target signals in multiple input multiple output (MIMO) communication systems. However, a single receiver antenna is favored for many practical applications due to size, power, and cost constraints. Consequently, further work is needed to address the important practical problems of classifying signals with a single receiver antenna.

Space–time block coding is a practical signal design technique aimed at capitalizing on the theoretical information capacity of MIMO channels.[1] MIMO communication systems accompanied by space–time block codes (STBCs) have been standardized in IEEE 802.16e and IEEE 802.11n, and appear to be ideal technologies for the next generation of wireless communication. Consequently, the blind classification of

* Corresponding author. Tel.: +86 535 6635871.
E-mail address: iamzlm@163.com (L. Zhang).

Peer review under responsibility of Editorial Committee of CJA.

ELSEVIER Production and hosting by Elsevier

http://dx.doi.org/10.1016/j.cja.2016.04.006

STBCs is a key research issue in non-cooperative MIMO-STBC communication systems and can be divided into four categories: maximum likelihood,[2,3] second-order statistics,[4–8] cyclostationarity-based[9–12] and fourth-order statistics.[13–15] Maximum likelihood algorithms employ the maximum likelihood criterion to find optimum solutions. However, their computational complexity is too high for higher order modulation, and they require a priori information, such as channel coefficients, modulation scheme, carrier frequency offset and carrier phase.[2,3] Second-order statistics is a method based on the space–time correlation of received signals to classify the STBCs in multiple receiver antennas systems.[4–8] In Refs. [9–12], the cyclostationarity properties of received signals are exploited for the classification of STBCs in the context of multiple receiver antennas. The fourth-order statistical method uses the fourth-order statistics of received signals as discriminating signal features to classify the STBCs with a single receiver antenna[14,15] or to estimate channel coefficients.[13] However, except for Refs. [14,15], most previous research[3–15] focuses on the context of multiple receiver antennas. Therefore, further work is needed to address the practical problem of classifying the STBCs with a single receiver antenna. In this paper, we propose a STBCs classification algorithm based on fourth-order cumulants with a single receiver antenna over frequency-flat Nakagami-m fading channels.[16] This algorithm does not require any a priori information of modulation scheme, channel coefficients or noise power. Consequently, it is well suited for non-cooperative scenarios.

Three distinct differences exist between the proposed method and those found in Refs. [14,15] First, fourth-order cumulants are employed in this paper, however, fourth-order moment (FOM) and the discrete fourier transform (DFT) of the fourth-order lag product (FOLP) are used in the literature.[14,15] The fourth-order cumulants of zeros-mean Gaussian white noise are equal to zero and the fourth-order moment is not equal to zero. Theoretically, we can ignore the effect of the Gaussian white noise in the derivation of theoretical value of the fourth-order cumulants. This explains why the proposed algorithm performs better than other methods in Refs. [14,15] at a low SNR. Second, the proposed algorithm can classify general STBCs while those in Ref. [14] only distinguish Alamouti coding from spatial multiplexing(SM). Moreover, Spatial Multiplexing cannot be categorized into the STBCs. Finally, the fourth-order lag cumulants of STBCs present non-null values that depend on the transmitted STBCs. The FOM-based algorithm employs the likelihood ratio test for decision making. The FOLP-based algorithm detects the peaks or the position of the peaks within the frequency domain of the fourth-order lag product in Refs. [14,15]

The rest of this paper is organized as follows: Section 2 – signal model and assumptions; Section 3 – the derivation of the fourth-order cumulants of STBCs; Section 4 – the proposed STBCs classification algorithm; Section 5 – simulation results; Section 6 – conclusions.

2. Signal model and assumptions

Let us consider a wireless communication system composed of a single receiver antenna and N_t transmit antennas. We assume the symbols that belong to the same complex linear modulation are independent and identically distributed (i.i.d) random variables. For quadrature phase shift keying(QPSK) constellation, the real and imaginary parts of the transmitted symbols are also i.i.d. That is to say, $E(|x|^2)=1$ and $E(x^2)=E[(x^*)^2]=0$.

$$E(x^4)=E[(x^*)^4]=-1 \tag{1}$$

The N transmitted symbols can be divided into blocks with length of N_s. Each block of N_s modulated symbols is encoded to generate N_t parallel signal sequences of length L. The kth block of N_s transmitted complex symbols is denoted by $\boldsymbol{X}_k=[x_{k,0},x_{k,1},\cdots,x_{k,N_t-1}]$.

(1) For SM, a block of $N_s=N_t$ symbols is transmitted through N_t antennas in a single time period ($L=1$). The corresponding coding matrix can be given as

$$\boldsymbol{G}^{\mathrm{SM}}(\boldsymbol{X}_k)=\boldsymbol{X}_k=[x_{k,0},x_{k,1},\cdots,x_{k,N_t-1}]^{\mathrm{T}} \tag{2}$$

(2) For Alamouti coding (Al), a block of $N_s=2$ symbols is transmitted through 2 antennas in two consecutive time periods ($L=2$). Alamouti coding is an orthogonal STBC(OSTBC). The corresponding coding matrix can be given as:[17]

$$\boldsymbol{G}^{\mathrm{Al}}(\boldsymbol{X}_k)=\begin{bmatrix} x_{k,0} & -x_{k,1}^* \\ x_{k,1} & x_{k,0}^* \end{bmatrix} \tag{3}$$

where $*$ represents complex conjugate.

(3) For OSTBC-3/4 coding (ST3), a block of $N_s=3$ symbols is transmitted through 3 antennas in four consecutive time periods ($L=4$). The OSTBC-3/4 coding is also an orthogonal STBC. The corresponding coding matrix can be given as:[1]

$$\boldsymbol{G}^{\mathrm{ST3}}(\boldsymbol{X}_k)=\begin{bmatrix} x_{k,0} & 0 & x_{k,1} & -x_{k,2} \\ 0 & x_{k,0} & x_{k,2}^* & x_{k,1}^* \\ -x_{k,1}^* & -x_{k,2} & x_{k,0}^* & 0 \end{bmatrix} \tag{4}$$

(4) For OSTBC-1/2 coding (ST4), a block of $N_s=4$ symbols is transmitted through 3 antennas in eight consecutive time periods ($L=8$). The OSTBC-1/2 coding is also an orthogonal STBC. The corresponding coding matrix can be given as:[18]

$$\boldsymbol{G}^{\mathrm{ST4}}(\boldsymbol{X}_k)=\begin{bmatrix} x_{k,0} & -x_{k,1} & -x_{k,2} & -x_{k,3} & x_{k,0}^* & -x_{k,1}^* & -x_{k,2}^* & -x_{k,3}^* \\ x_{k,1} & x_{k,0} & x_{k,3} & -x_{k,2} & x_{k,1}^* & x_{k,0}^* & x_{k,3}^* & -x_{k,2}^* \\ x_{k,2} & -x_{k,3} & x_{k,0} & x_{k,1} & x_{k,2}^* & -x_{k,3}^* & x_{k,0}^* & x_{k,1}^* \end{bmatrix} \tag{5}$$

Let us consider a receiver with a single antenna. The length and start of STBCs are unknown at the receiver side in a non-cooperative scenario. The first received column is expressed as $r(0)$, so the $(k+1)$ th intercepted column $r^{\lambda}(k)$ can be denoted as

$$r^{\lambda}(k)=\boldsymbol{H}\boldsymbol{S}(k)+w(k)=Y(k)+w(k) \tag{6}$$

where $\boldsymbol{S}(k)=\boldsymbol{G}_p^{\lambda}(\boldsymbol{X}_q)$, with $p=(k+k_1)\mathrm{mod}L$, $q=(k+k_1)\,\mathrm{div}L$, $0\leqslant k_1<L$, and $\lambda\in\Omega$, $\Omega\in\{\mathrm{SM},\mathrm{Al},\mathrm{ST3},\mathrm{ST4}\}$. $w(k)$ denotes complex Gaussian white noise with zero-mean and variance σ_w^2. It is worth noting that the additive noise is supposed to be Gaussian complex circular and temporally uncor-

related. $\boldsymbol{H} = [h_0, h_1, \cdots, h_{N_t-1}]$ denotes the vector of the fading channel coefficients, which is constant over the observation period.

In this paper, we resort to using fourth-order cumulants to blindly classify the proposed STBCs above from K received columns when a single receiver antenna is available. More details are in the next section.

3. The fourth-order cumulants of STBCs

In this section, the expression of fourth-order cumulants is deduced in order to discover the characteristic parameters that can blindly classify STBCs in a non-cooperative scenario.

3.1. Principles

For the complex-value stationary random process $r(k)$, second-order moments can be defined in two different ways:

$$\begin{cases} C_{20} = E[r(k)^2] \\ C_{21} = E[|r(k)|^2] \end{cases} \tag{7}$$

Similarly, fourth-order cumulants can be defined in three ways:

$$\begin{cases} C_{40} = \mathrm{cum}(r(k), r(k), r(k), r(k)) \\ C_{41} = \mathrm{cum}(r(k), r(k), r(k), r(k)^*) \\ C_{42} = \mathrm{cum}(r(k), r(k), r(k)^*, r(k)^*) \end{cases} \tag{8}$$

where, the statistics in Eqs. (7) and (8) are the zeroth lags of the correlations and fourth-order cumulants of $r(k)$, For zero-mean w, x, y, and z,the fourth-order cumulants can be defined as

$$\begin{aligned} \mathrm{cum}(w, x, y, z) = {} & E(wxyz) - E(wx)E(yz) - E(wy)E(xz) \\ & - E(wz)E(xy) \end{aligned} \tag{9}$$

If random variable x_i and y_i are statistically independent, the cumulants have the characteristics of half-invariance, so

$$\begin{aligned} & \mathrm{cum}(x_1 + y_1, x_2 + y_2, \cdots, x_k + y_k) \\ & = \mathrm{cum}(x_1, x_2, \cdots, x_k) + \mathrm{cum}(y_1, y_2, \cdots, y_k) \end{aligned} \tag{10}$$

3.2. The derivation of the fourth-order cumulants for STBCs

Eqs. (6) and (10) can be deduced as

$$C^{\lambda}_{40,r(k)} = \mathrm{cum}(Y(k)Y(k+\tau_1)Y(k+\tau_2)Y(k+\tau_3)) \tag{11}$$

In Refs. [19,20], the fourth order cumulants of zeros-mean Gaussian white noise are equal to zero, but the fourth order moments are not equal to zero. Therefore, we choose fourth-order cumulants as a tool to blindly classify the STBCs. Eq. (11) can be simplified as

$$\begin{aligned} C^{\lambda}_{40,r(k)} &= \mathrm{cum}[Y(k)Y(k+\tau_1)Y(k+\tau_2)Y(k+\tau_3)] \\ &= E[Y(k)Y(k+\tau_1)Y(k+\tau_2)Y(k+\tau_3)] \\ &\quad - E[Y(k)Y(k+\tau_1)]E[Y(k+\tau_2)Y(k+\tau_3)] \\ &\quad - E[Y(k)Y(k+\tau_2)]E[Y(k+\tau_1)Y(k+\tau_3)] \\ &\quad - E[Y(k)Y(k+\tau_3)]E[Y(k+\tau_1)Y(k+\tau_3)] \end{aligned} \tag{12}$$

where $\tau_1 = 0$ and $\tau_2 = \tau_3 \in \{1, 2, 5\}$.

Therefore, the fourth-order cumulants of ST4 at a delay-vector $[0, 0, 1, 1]$ can be expressed as

$$\begin{aligned} C^{\mathrm{ST4}}_{40,r(k)} &= \mathrm{cum}[Y(k)Y(k)Y(k+1)Y(k+1)] \\ &= E[Y^2(k)Y^2(k+1)] - E[Y^2(k)]E[Y^2(k+1)] \\ &\quad - 2E([Y(k)Y(k+1)])^2 \\ &= \frac{1}{8}(4E(h_0^2h_1^2x^4) + 2E(h_1^2h_2^2(|x|^4 - 2|x|^2|x|^2))) \\ &\quad + \frac{1}{8}(2E(h_1^2h_2^2x^4) + 4E(h_1^2h_0^2(x^*)^4) + 2E(h_1^2h_2^2(x^*)^4)) \end{aligned} \tag{13}$$

where h_i represents the channel coefficient between the i transmit antenna and receive antenna.

The fourth-order cumulants of ST4 at a delay-vector $[0, 0, 2, 2]$ can be expressed as

$$\begin{aligned} C^{\mathrm{ST4}}_{40,r(k)} &= \mathrm{cum}[Y(k)Y(k)Y(k+2)Y(k+2)] \\ &= E[Y^2(k)Y^2(k+2)] - E[Y^2(k)]E[Y^2(k+2)] \\ &\quad - 2E([Y(k)Y(k+2)])^2 \\ &= \frac{1}{8}(4E(h_0^2h_2^2(|x|^4 - 2|x|^2|x|^2)) + 4E(h_0^2h_2^2x^4) \\ &\quad + 4E(h_0^2h_2^2(x^*)^4)) \end{aligned} \tag{14}$$

The fourth-order cumulants of ST4 at a delay-vector $[0, 0, 5, 5]$ can be expressed as

$$\begin{aligned} C^{\mathrm{ST4}}_{40,r(k)} &= \mathrm{cum}[Y(k)Y(k)Y(k+5)Y(k+5)] \\ &= E[Y^2(k)Y^2(k+5)] - E[Y^2(k)]E[Y^2(k+5)] \\ &\quad - 2E([Y(k)Y(k+5)])^2 \\ &= \frac{1}{8}(4E(h_0^2h_2^2(|x|^4 - 2|x|^2|x|^2)) \\ &\quad + 2E(h_1^2h_2^2(|x|^4 - 2|x|^2|x|^2))) \end{aligned} \tag{15}$$

The fourth-order cumulants of SM, Al and ST3 at different delay-vectors can be obtained in similar ways.

For SM, the transmitted symbols are independent in different time slots. Therefore, the fourth-order cumulants of SM are equal to zero at different delay-vectors.

$$C^{\mathrm{SM}}_{40,r(k)}[0, 0, 1, 1] = C^{\mathrm{SM}}_{40,r(k)}[0, 0, 2, 2] = C^{\mathrm{SM}}_{40,r(k)}[0, 0, 5, 5] \tag{16}$$

The fourth-order cumulants of Al at different delay-vectors can be deduced as follows:

(1) The fourth-order cumulants of Al at a delay-vector $[0, 0, 1, 1]$ are expressed as

$$\begin{aligned} C^{\mathrm{Al}}_{40,r(k)} &= \mathrm{cum}[Y(k)Y(k)Y(k+1)Y(k+1)] \\ &= E[(h_0x_{c,0} + h_1x_{c,1})^2(-h_0x^*_{b,1} + h_1x^*_{b,0})^2] \\ &\quad - E[(h_0x_{c,0} + h_1x_{c,1})^2] \\ &\quad E[(-h_0x^*_{b,1} + h_1x^*_{b,0})^2] \\ &\quad - 2E[(h_0x_{c,0} + h_1x_{c,1})(-h_0x^*_{b,1} + h_1x^*_{b,0})]^2 = C \end{aligned} \tag{17}$$

where $x_{c,0}$ represents the zeroth transmit symbol in the cth coding matrix. If $c \neq b$, it represents symbol $x_{c,0}$ and $x_{b,0}$ are not in the same coding matrix.If $c = b$, C can be expresses as

$$C = 2E[(h_0^2h_1^2(|x|^4 - 2|x|^2|x|^2))] \tag{18}$$

Else

$$C = 0 \tag{19}$$

Therefore, $C^{\mathrm{Al}}_{40,r(k)}$ can be expressed as

$$\begin{aligned} C^{\mathrm{Al}}_{40,r(k)} &= 2 \times 0.5 \times E[h_0^2 h_1^2 (|x|^4 - 2|x|^2|x|^2)] \\ &= E(h_0^2 h_1^2 C_{42,x}) \end{aligned} \tag{20}$$

(2) As the length of the code matrix is equal to 2, the transmitted symbols in a different code matrix are independent. The fourth-order cumulants of Al are equal to zero at delay-vectors $[0,0,2,2]$ and $[0,0,5,5]$.

$$C^{\mathrm{Al}}_{40,r(k)}[0,0,2,2)] = C^{\mathrm{Al}}_{40,r(k)}[0,0,5,5] = 0 \tag{21}$$

The fourth-order cumulants of ST3 at different delay-vectors can be deduced as follows:

(1) The fourth-order cumulants of ST3 at a delay-vector $[0,0,1,1]$ are expressed as

$$\begin{aligned} C^{\mathrm{ST3}}_{40,r(k)} &= \mathrm{cum}[Y(k)\,Y(k)\,Y(k+1)\,Y(k+1)] \\ &= E[Y^2(k)\,Y^2(k+1)] - E[Y^2(k)]E[Y^2(k+1)] \\ &\quad - 2E([Y(k)\,Y(k+1)])^2 \\ &= \frac{1}{4}\{E(h_0^2 h_1^2 x^4) + 2E[h_1^2 h_2^2 (|x|^4 - 2|x|^2|x|^2)] \\ &\quad + 2E[h_0^2 h_1^2 (|x|^4 - 2|x|^2|x|^2)]\} \end{aligned} \tag{22}$$

(2) The fourth-order cumulants of ST3 at a delay-vector $[0,0,2,2]$ are expressed as

$$\begin{aligned} C^{\mathrm{ST3}}_{40,r(k)} &= \mathrm{cum}[Y(k)\,Y(k)\,Y(k+2)\,Y(k+2)] \\ &= E[Y^2(k)\,Y^2(k+2)] - E[Y^2(k)]E[Y^2(k+2)] \\ &\quad - 2E([Y(k)\,Y(k+2)])^2 \\ &= \frac{1}{4}\{E(h_0^2 h_1^2 x^4) + 2E[h_0^2 h_2^2 (|x|^4 - 2|x|^2|x|^2)]\} \end{aligned} \tag{23}$$

(3) As the length of the code matrix is equal to 4, the fourth-order cumulants of ST3 at a delay-vector $[0,0,5,5]$ are equal to zero.

$$C^{\mathrm{ST3}}_{40,r(k)}[0,0,5,5] = 0 \tag{24}$$

Examples of moments and cumulants corresponding to different signal constellations are provided in Table 1. In Table 1, PSK refers to phase shift keying, QAM refers to quadrature amplitude modulation, and QPSK refers to quad.

Where $m_{\alpha\beta,x} = E(x^{\alpha-\beta}(x^*)^{\beta})$ denotes the (α,β) moment corresponding to the signal constellation. $C_{42,x} = E(|x|^4) - 2(E(|x|^2))^2$ and $C_{21,x} = E(|x|^2)$ represent the $(4,2)$ cumulant and $(2,1)$ cumulant corresponding to the signal constellation respectively.

Table 1 Moments and cumulants values for various signal constellations.

Parameter	QPSK	8PSK	16-QAM	64-QAM
$m_{21,x} = C_{21,x}$	1	1	1	1
$C_{42,x}$	−1	−1	−0.68	−0.619

The conclusion in Section 3 can be reached that the fourth-order cumulants at different time delays-vectors present non-null values that depend on the transmitted STBCs. For QPSK modulation, the theoretical values of the fourth-order cumulants for SM, Al, ST3 and ST4 are provided in Table 2.

4. Blind classification of STBCs by decision tree and hypothesis testing

In this section, we propose a classifier for blind recognition of 4 linear STBCs, which are introduced above. The automatic classification of these STBCs is accomplished by using a decision tree.

4.1. The estimated values of fourth-order cumulants

In the practical applications of signal processing, the fourth-order cumulants can be estimated from the limited length received signals. Given the observed data $r(k), k = 1,2,\ldots,K$, the estimation of the fourth-order cumulants can be expressed as

$$\begin{aligned} \hat{C}_{40,r(k)} &= \hat{m}_{40,r(k)}(\tau_1,\tau_2,\tau_3) - \hat{R}_{r(k)}(\tau_1)\hat{R}_{r(k)}(\tau_3-\tau_2) \\ &\quad - \hat{R}_{r(k)}(\tau_2)\hat{R}_{r(k)}(\tau_3-\tau_1) - \hat{R}_{r(k)}(\tau_3)\hat{R}_{r(k)}(\tau_2-\tau_1) \end{aligned} \tag{25}$$

where $\hat{R}_{r(k)}(\tau_1)$ can be defined as

$$\hat{R}_{r(k)}(\tau_1) = m_{r(k)}(\tau_1) = \frac{1}{K}\sum_{i=0}^{K-1} r(i)r(i+\tau_1) \tag{26}$$

By using Eqs. (25) and (26), $\hat{C}_{40,r(k)}$ can be obtained as

$$\begin{aligned} \hat{C}_{40,r(k)} &= \hat{m}_{40,r(k)}(\tau_1,\tau_2,\tau_3) - \hat{m}_{r(k)}(\tau_1)\hat{m}_{r(k)}(\tau_3-\tau_2) \\ &\quad - \hat{m}_{r(k)}(\tau_2)\hat{m}_{r(k)}(\tau_3-\tau_1) - \hat{m}_{r(k)}(\tau_3)\hat{m}_{r(k)}(\tau_2-\tau_1) \\ &= \frac{1}{K}\sum_{i=0}^{K-1} r(i)r(i+\tau_1)r(i+\tau_2)r(i+\tau_3) \\ &\quad - \frac{1}{K^2}\sum_{i=0}^{K-1} r(i)r(i+\tau_1)\sum_{i=0}^{K-1} r(i)r(i) + (\tau_3-\tau_2) \\ &\quad - \frac{1}{K^2}\sum_{i=0}^{K-1} r(i)r(i+\tau_2)\sum_{i=0}^{K-1} r(i)r(i) + (\tau_3-\tau_1) \\ &\quad - \frac{1}{K^2}\sum_{i=0}^{K-1} r(i)r(i+\tau_3)\sum_{i=0}^{K-1} r(i)r(i) + (\tau_2-\tau_1) \end{aligned} \tag{27}$$

Table 2 Theoretical values of the fourth-order cumulants $C_{40,r(k)}$ at different delay vectors (QPSK modulation).

STBCs	$C_{40,r(k)}$	
	$\tau_1 = 0, \tau_2 = \tau_3$	$C_{42,r(k)}$
SM	1	0
	2	0
	5	0
Al	1	1
	2	0
	5	0
ST3	1	1.25
	2	0.75
	5	0
ST4	1	1.75
	2	1.50
	5	0.75

4.2. Decision tree

From transmission, the theoretical values of fourth-order cumulants are obtained due to the derivation in Section 3. For the 4 STBCs under consideration, the theoretical values of fourth-order cumulants are reported on Table 2. By analyzing Table 2, we propose a new method to blindly classify the STBCs with the decision tree in Fig. 1. The ST4 is recognized by the non-null value of fourth-order cumulants at delay-vector $[0,0,5,5]$. The presence of the ST3 is then detected from the non-null value of the fourth-order cumulants at delay-vector $[0,0,2,2]$. Subsequently, the fourth-order cumulants at delay-vector $[0,0,1,1]$ are used to discriminate Al from SM. At each node of the tree, the nullity of $\hat{C}_{40,r(k)}$ is tested. In an experiment, $\hat{C}_{40,r(k)}$ can be estimated and the test of nullity accomplished by a hypothesis testing.

4.3. Detection of null values using hypothesis testing

From the data in Table 2, we propose a new method to blindly classify the STBCs by detecting the non-null value of the fourth-order cumulants at different delay vectors. The detection of the non-null values can be performed by the following hypothesis testing:

Hypothesis H_0: $\hat{C}_{40,r(k)} = 0$
Hypothesis H_1: $\hat{C}_{40,r(k)} \neq 0$

According to central limit theorem, $\hat{C}_{40,r(k)}$ is an asymptotically normal estimator of $\hat{C}_{40,r(k)}$. The interceptor is composed of a single receiver antenna. Fig. 2 presents a histogram of $\hat{C}_{40,r(k)}$ for a wireless communication using ST3 and QPSK modulation.

The fourth-order cumulants $\hat{C}_{40,r(k)}$ are subjected to an asymptotically normal distribution under assumption H_0. The knowledge of the distribution of $\hat{C}_{40,r(k)}$ under assumption H_0 permits one to set the threshold. The threshold, ξ, is obtained from the probability of false alarm(PFA), defined by:

$$\mathrm{PFA} = \int_{\xi}^{\infty} \sqrt{\frac{1}{2\pi\delta^2}} \mathrm{e}^{\frac{-(x-\mu)^2}{2\delta^2}} \mathrm{d}x \tag{28}$$

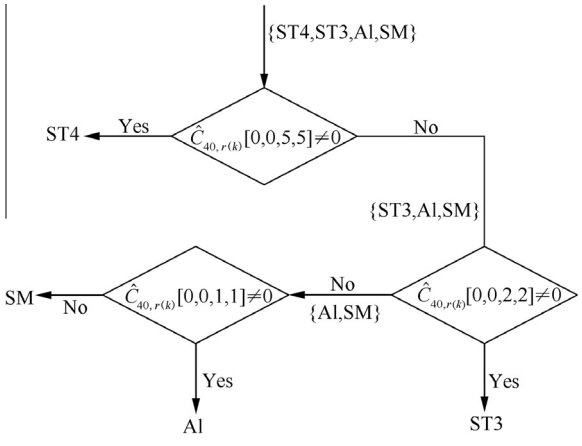

Fig. 1 Decision tree for classification of 4 STBCs.

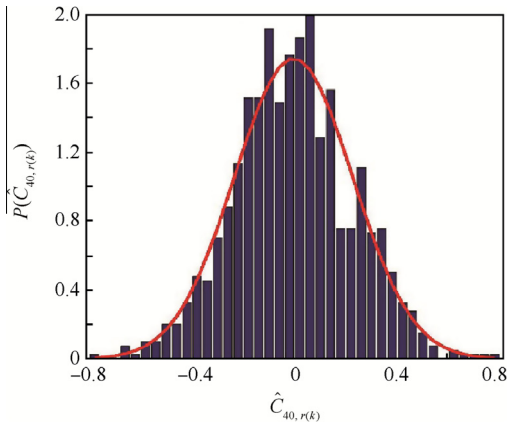

Fig. 2 Distribution of $\hat{C}_{40,r(k)}$ of STBCs at delay-vector $[0,0,2,2]$ at SNR = 20 dB.

where, under assumption H_0, μ and δ are mean value and variance respectively. Taking the inverse function of Eq. (28) leads to ξ. Hypothesis H_0 is selected if $\hat{C}_{40,r(k)} < \xi$, otherwise, hypothesis H_1 is selected.

The average probability of correct classification $p(\lambda|\lambda)$, can be expressed as

$$P_{\mathrm{c}} = \frac{1}{4}\sum_{\lambda\in\Omega} p(\lambda|\lambda) \tag{29}$$

5. Simulation results

5.1. Simulation setup

1000 Monte Carlo trials were performed to evaluate the performance of the proposed algorithm. SM, Al, ST3 and ST4 were considered in simulations. Unless specifically indicated, QPSK modulation was used where $K = 8192$ and $\mathrm{PFA} = 10^{-2}$. The received signal was affected by additive white Gaussian noise (AWGN) with variance σ_{w}^2. Channel was set to a frequency-flat Nakagami-m fading channel, with $m = 3$ and $E(|h_i|^2) = 1, i = 0,1,2,3$. SNR was set to $10\lg\left(\frac{N_{\mathrm{t}}}{\sigma_{\mathrm{w}}^2}\right)$. Two performance measures were used: the average probability of correct classification, which was addressed in Eq. (29), and the probability of correct classification $p(\lambda|\lambda), \lambda \in \Omega$.

5.2. Performance evaluation

Fig. 3 presents the simulation results for the probability of correct classification over the Nakagami-m fading channel for $m = 3$ .Note that the probability of correct classification for Al, ST3 and ST4 is dependent on SNRs but not SM. For Al, the probability of correct classification is close to 1 at a SNR equal to −3 dB. For ST3, the probability of correct classification is close to 1 at a SNR equal to 2 dB. For ST4, the probability of correct classification is close to 1 at a SNR equal to 6 dB. Therefore, the proposed algorithm performs well in low SNR scenarios. Al shows better performance than ST3 and ST4 at a low SNR. The fourth-order cumulants of Al, ST3 and SM are subject to Gaussian distribution at delay-vector $[0,0,5,5]$ and their trails have some overlap on the distribution

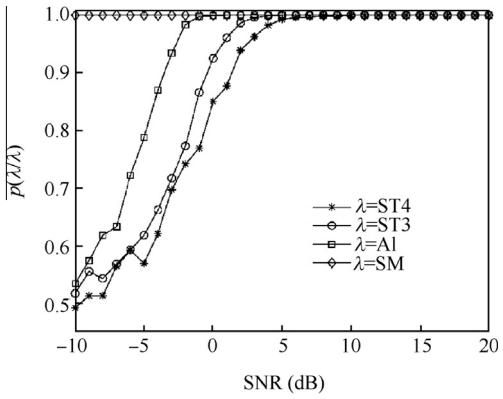

Fig. 3 Probability of correct classification $p(\lambda|\lambda)$.

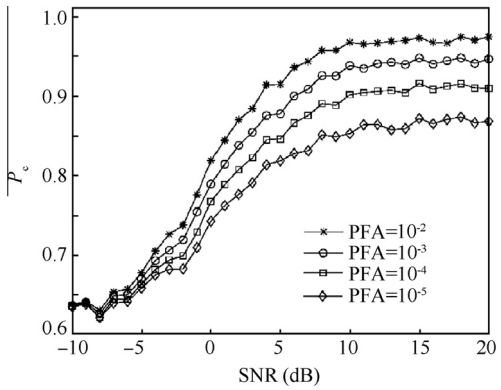

Fig. 5 Effect of the probability of false alarm on P_c.

of $\hat{C}_{40,r(k)}$ of ST4. Therefore, in the hierarchical recognition of STBCs, the recognition of ST4 at first node is disturbed due to the existence of the other STBCs.

5.3. Influence of the number of received samples K

Fig. 4 illustrates the classification behavior of a single receiver antenna interceptor with received samples equal to 8192, 4096, 2048, 1024 and 512 respectively. The simulation conditions as follows: the SM, Al, ST3 and ST3 are under consideration and PFA $= 10^{-2}$. In each case, the average probability of correct classification reaches its maximum at a SNR equal to 5 dB. With $K = 8192$, the average probability of correct classification shows better performance at a SNR less than 5 dB. With $K = 8192$, the average probability of correct classification is close to 1 at a SNR equal to 4 dB. The average probability of correct classification is enhanced by a greater number of received samples. This improvement is due to a more accurate estimation of the fourth-order cumulants $\hat{C}_{40,r(k)}$.

5.4. Influence of the probability of false alarm

Fig. 5 presents the performance of the proposed algorithm with respect to the probability of false alarm with a single receiver antenna interceptor receiving 2048 samples. In four cases, the average probability of correct classification shows better performance when the probability of false alarm equals 10^{-2}. The analysis is described as follows: $\hat{C}_{40,r(k)}$ is a Gaussian distribution; higher probability of false alarm leads to a lower threshold, therefore, the range of the interval $[\mu + \xi, 2\mu - \xi]$ is enlarged and the performance of classification is enhanced.

5.5. Influence of the modulation scheme

We have illustrated the behavior of a proposed algorithm for four complex modulation schemes: 16-QAM, 64-QAM, 8-PSK and QPSK. The simulation conditions as follows: the SM, Al, ST3 and ST3 are under consideration, PFA $= 10^{-2}$, $K = 2048$ and $m = 3$. Fig. 6 shows performance with respect to modulation scheme. We find that classification performance is dependent on the M-QAM modulation but not M-PSK modulation. The explanation for this phenomenon concerning modulation scheme is described as follows: According to Section 3, the performance of the proposed algorithm is determined by the Euclidean distance between the fourth-order cumulants $\hat{C}_{40,r(k)}$ and zero, which improves as the distance increases. The fourth-order cumulants are related to $C_{42,x}$, which increases as $C_{42,x}$ increases. $C_{42,x}$ is independent on the M-PSK constellations, whereas it decreases as M increases for M-QAM constellations.

5.6. Influence of m for Nakagami-m channel

Fig. 7 presents the performance of the proposed algorithm with respect to m for an interceptor with a single receiver antenna and 2048 samples. The simulation conditions as

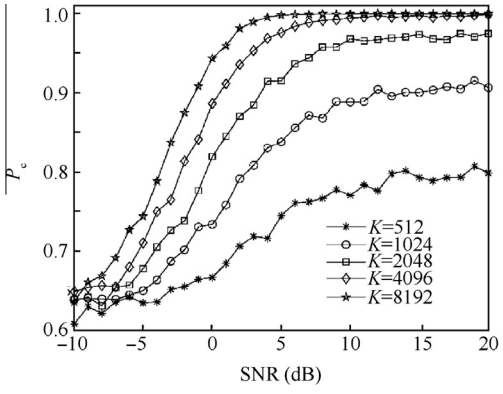

Fig. 4 Effect of the number of received samples K on P_c .

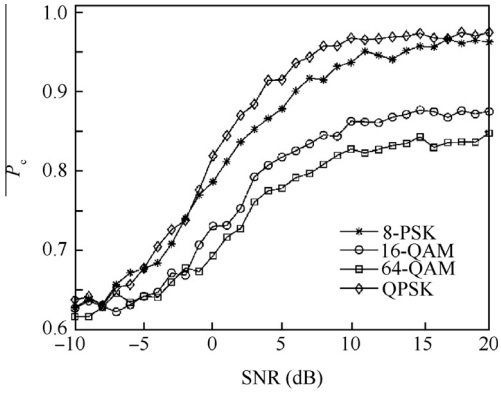

Fig. 6 Effect of the modulation scheme on P_c.

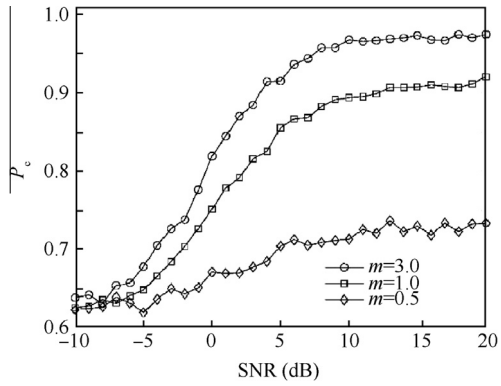

Fig. 7 Effect of m on P_c.

follows: the SM, Al, ST3 and ST3 are under consideration and PFA $= 10^{-2}$ .The variance of the channel coefficients increases for lower m values, which affects the value of the variance of $\hat{C}_{40,r(k)}$, thus leading to erroneous results.

5.7. Performance comparison

Fig. 8 compares the average probability of correct classification with the algorithms mentioned in Refs. [14,15] FOLP-A, FOLP-B and FOLP-C represent these algorithms in Refs. [14], respectively. These algorithms[14,15] are sensitive to Gaussian noise and perform unsatisfactory at a SNR less than 5 dB. In addition, the algorithms mentioned in Ref. [14] merely discriminate between spatial multiplexing and Alamouti coding. The proposed algorithm performs well even at a SNR equal to 0 dB. This is due to the employment of the fourth-order cumulants, which are not sensitive to Gaussian noise.

We compare the performance of the proposed method with algorithms in Refs. [14,15] in detail below. The simulation conditions are different than in the Refs. [14,15] Ref. [14] investigated SM and Al signals for classification, and it did not involve the general STBCs. Ref. [15] investigated 4 STBCs. Table 3 and Table 4 compare the average probability of correct classification P_c, over Nakagami-m fading channel, $m = 3$, for different values of SNR of the proposed algorithm and those algorithms in Refs. [14,15] For Table 3 and Table 4, the number of symbols are set to 1024 and 8192 respectively. The proposed algorithm exhibits superior performance, especially at a lower SNR.

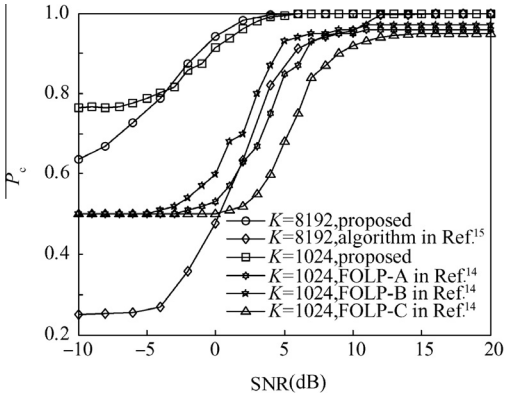

Fig. 8 Comparison of algorithms in Refs. [14,15]

Table 3 Effect of SNR on P_c for proposed algorithm, FOLP-A, FOLP-B, and FOLP-C.

SNR(dB)	P_c			
	Proposed algorithm	FOLP-A	FOLP-B	FOLP-C
−10	0.7640	0.5000	0.5000	0.5000
−5	0.7880	0.5100	0.5100	0.5100
0	0.9570	0.5250	0.6000	0.5100
5	0.9970	0.8500	0.9100	0.6700
10	1.0000	0.9600	1.0000	0.9250
15	1.0000	1.0000	1.0000	0.9220
20	1.0000	1.0000	1.0000	0.9300

Table 4 Effect of SNR on P_c for proposed algorithm and algorithm in Ref. [15]

SNR(dB)	P_c	
	Proposed algorithm	Algorithm in Ref. [15]
−10	0.6375	0.2510
−5	0.7543	0.2530
0	0.9555	0.4521
5	0.9988	0.8610
10	1.0000	0.9920
15	1.0000	1.0000
20	1.0000	1.0000

In Table 5 and Table 6, the effect of the number of received symbols K on P_c at SNR = 10 dB is presented for the proposed algorithm and the algorithms in Refs. [14,15] Increasing the number of symbols results in a performance improvement for the proposed algorithm due to a more accurate estimate of the fourth-order cumulants $\hat{C}_{40,r(k)}$. It is worth noting that the proposed algorithm outperforms those in Refs. [14,15]

Table 7 and Table 8 present the modulation scheme effect on P_c at SNR = 10 dB for the proposed algorithm and the algorithms in Refs. [14,15] The proposed algorithm is independent of M for the M-PSK modulation ($M \geqslant 4$); it degrades slightly as M increase for M-QAM modulation. It should also be noted that less K is needed to attain a classification performance for M-PSK ($M \geqslant 4$) similar to that for M-QAM modulation. For example, for $K = 2048$, $P_c = 0.9980$ and $P_c = 0.9940$ for the proposed algorithm, while $P_c = 0.8500$ and $P_c = 0.7800$ results from FOLP-C with 16-QAM and 64-QAM respectively. Therefore, the proposed algorithm outperforms those in Refs. [14,15](see Tables 7 and Table 8).

Table 9 and Table 10 present the effect of m on P_c at SNR = 10 dB for the proposed algorithm and the algorithms in Refs. [14,15] The proposed algorithm exhibits a lower sensitivity to m when compared with the algorithms in the Refs. [14,15]

Table 5 Effect of the number of symbols on P_c for proposed algorithm, FOLP-A, FOLP-B, and FOLP-C.

K	P_c			
	Proposed algorithm	FOLP-A	FOLP-B	FOLP-C
512	0.9908	0.9600	0.9500	0.8300
1024	1.0000	0.9700	0.9700	0.9300
2048	1.0000	0.9800	0.9800	0.9800
4096	1.0000	1.0000	1.0000	1.0000

Table 6 Effect of the number of symbols on P_c for proposed algorithm and algorithm in Ref. [15]

K	P_c	
	Proposed algorithm	Algorithm in Ref. [15]
2048	0.9680	0.8650
4096	0.9948	0.9452
8192	1.0000	0.9900

Table 7 Effect of modulation scheme on P_c for proposed algorithm, FOLP-A, FOLP-B, and FOLP-C.

Modulation	P_c			
	Proposed algorithm	FOLP-A	FOLP-B	FOLP-C
QPSK	1.0000	0.9900	0.9900	0.9800
8-PSK	1.0000	0.9900	0.9900	0.9800
16-QAM	0.9980	0.9600	0.9800	0.8500
64-QAM	0.9940	0.9400	0.9700	0.7800

Table 8 Effect of modulation scheme on P_c for proposed algorithm and algorithm in Ref. [15]

Modulation	P_c	
	Proposed algorithm	Algorithm in Ref. [15]
QPSK	1.0000	0.9910
8-PSK	0.9933	0.9910
16-QAM	0.9400	0.8980
64-QAM	0.9320	0.8950

Table 9 Effect of the Nakagami-m on P_c for proposed algorithm, FOLP-A, FOLP-B, and FOLP-C.

m	P_c			
	Proposed algorithm	FOLP-A	FOLP-B	FOLP-C
1	0.9835	0.8400	0.8750	0.7500
3	1.0000	0.9900	0.9500	0.9050

Table 10 Effect of the Nakagami-m on P_c for proposed algorithm and algorithm in Ref. [15]

m	P_c	
	Proposed algorithm	Algorithm in Ref. [15]
1	0.9958	0.8750
3	1.0000	0.9870

Table 11 Effect of PFA on P_c for proposed algorithm and FOLP-A.

PFA	P_c	
	Proposed algorithm	FOLP-A
10^{-2}	1.0000	1.0000
10^{-3}	1.0000	1.0000
10^{-4}	0.9970	1.0000
10^{-5}	0.9875	1.0000

Table 11 presents the effect of PFA on P_c at SNR = 10 dB for the proposed algorithm and the algorithm in Ref. [14] The two algorithms exhibit similar performance.

6. Conclusions

This paper proposes a novel method for blind classification of STBCs based on the fourth-order cumulants. It shows that the fourth-order cumulants of the STBCs exhibit non-null values that depend on the transmitted STBCs. The detection of non-null values is performed through hypothesis testing, and automatic classification is done by decision tree. The proposed algorithm is evaluated for the classification of 4 STBCs with different code lengths: SM, Alamouti coding, and two kinds of orthogonal STBCs. The proposed algorithm operates well even at a low SNR with a single receiver antenna. The performance is enhanced by increasing the number of received samples. Additional experiments show that the probability of false alarm, modulation scheme and different Nakagami-m fading channels also influence the average probability of correct classification.

Acknowledgement

This study was co-supported by the Taishan Scholar Special Foundation of China (No. ts201511020).

References

1. Larsson E, Stoica P. *Space-time block coding for wireless communications*. Cambridge: Cambridge Press; 2003. p. 167–70.
2. Marey M, Dobre OA, Liao B. Classification of STBC systems over frequency-selective channels. *IEEE Transactions on Vehicular Technology* 2014;**64**(5):2159–64.
3. Choqueuse V, Marazin M. Blind recognition of linear space-time block codes: a likelihood-based approach. *IEEE Transactions on Signal Processing* 2010;**58**(3):1290–9.
4. Choqueuse V, Yao K. Hierarchical space-time block code recognition using correlation matrices. *IEEE Transactions on Wireless Communications* 2008;**7**(9):3526–34.
5. Choqueuse V, Yao K. *Blind recognition of linear space time block codes*. 2008 IEEE international conference on acoustics, speech and signal processing; 2008 Mar 31–April 4; Las Vegas, USA. Piscataway, NJ: IEEE Press; 2008. p. 2833–6.
6. Marey M, Dobre OA, Inkol R. Blind STBC identification for multiple antenna OFDM systems. *IEEE Transactions on Communications* 2014;**62**(5):1554–67.
7. Mohammadkarimi M, Dobre OA. Blind identification of spatial multiplexing and Alamouti space-time block code via Kolmogorov-Smirnov (K-S) test. *IEEE Communications Letters* 2014;**18**(10):1711–4.
8. Eldemerdash YA, Dobre OA, Liao BJ. Blind identification of SM and Alamouti STBC-OFDM signal. *IEEE Transactions on Wireless communications* 2015;**14**(2):972–82.
9. Shi M, BAR-NESS Y. *STC and BLAST MIMO modulation recognition. IEEE global telecommunications conference*; 2007 Nov 26–30; Washington D.C., USA. Piscataway, NJ: IEEE Press; 2007. p. 3034–9.
10. Marey M, Dobre OA. Classification of space-time block codes based on second-order cyclostationarity with transmission impairments. *IEEE Transactions on Wireless Communications* 2012;**11**(7):2574–84.
11. Karami E, Dobre OA. Identification of SM-OFDM and AL-OFDM signals based on their second-order cyclostationarity. *IEEE Transactions on Vehicular Technology* 2015;**64**(3):942–53.

12. De Young M, Heath R, Evans B. *Using higher order cyclostationarity to identify space-time block codes*. *IEEE global telecommunications conference*; 2008 Nov30–Dec4; New Orleans, USA. Piscataway, NJ: IEEE Press; 2008. p. 1–5.
13. Choqueuse V, Mansour A, Burel G. Blind channel estimation for STBC system using higher-order statistics. *IEEE Transactions on Wireless Communications* 2011;**10**(2):495–505.
14. Eldemerdash YA, Marey M, Dobre OA. Fourth-order statistics for blind classification of spatial multiplexing and Alamouti space-time block code signals. *IEEE Transactions on Communications* 2013;**5**(6):1–12.
15. Eldemerdash YA, Dobre OA, Marey M. *An efficient algorithm for space-time block code classification*. *IEEE Global Communication Conference*; 2013 Dec 9–13; Atlanta, USA. Piscataway, NJ: IEEE Press; 2013. p. 3034–9.
16. Beaulieu NC, Cheng C. Efficient Nakagami-*m* fading channel simulation. *IEEE Transactions on Vehicular Technology* 2005;**54**(2):413–24.
17. Alamouti A. A simple transmit diversity technique for wireless communication. *IEEE Journal on Selected Areas in Communications* 1998;**16**(8):1451–8.
18. Tarokh V, Jafarkhani H, Calderbank A. Space time block codes from orthogonal designs. *IEEE Transactions on Information Theory* 1999;**45**(5):1451–8.
19. Swami A, Sadler BM. Hierarchical digital modulation classification using cumulants. *IEEE Transactions on Communications* 2000;**48**(3):416–29.
20. Zhang XD. *Signal analysis and processing*. Beijing: Tsinghua University Press; 2011. p. 314–5.

Ling Qing is a Ph. D. student at Naval Aeronautical and Astronautical University. She received her M.E. degree from same University in 2012. Her areas of research include the blind identification of channel coding and Satellite reconnaissance.

Zhang Limin is a professor and Ph.D. supervisor at Naval Aeronautical and Astronautical University. He received the Ph.D. degree from the Tianjin University in 2005. His current research interests are the blind identification of channel coding and Satellite reconnaissance.

Yan Wenjun received M.E. and D.E. degrees from Naval Aeronautical and Astronautical University in 2015, and then became a teacher there. His main research interests are the blind identification of channel coding and Satellite reconnaissance.